EFFECT OF GAS FIELD PRODUCTION AND CO_2 INJECTION ON BRINE FLOW AND SALT PRECIPITATION

Tim Tambach[*], Daniël Loeve[*], Cor Hofstee[*], Willem-Jan Plug[**], and Jos Maas[*]

[*]TNO Geological Survey of the Netherlands, P.O. Box 80015, 3508 TA Utrecht, The Netherlands
[**]TAQA Energy B.V., P.O. Box 11550, 2502 AN, Den Haag, The Netherlands

e-mail: tim.tambach@tno.nl

ABSTRACT

This paper reports modeling of gas field production and CO_2 injection from a theoretical reservoir based on characteristics of the P18 gas field in the Dutch offshore, which consists of four geological deposits with different petrophysical properties. We especially focus on the brine flow during and after exploitation of the reservoir, which affects salt precipitation and dissolution in the near-well area. We first computed the water saturation (S_w) with depth, in static equilibrium with a free water level (FWL) at the bottom of the reservoir. We then computed production of the gas field, predicting a very low brine production and mobility, without salt precipitation. Subsequently, injection of dry CO_2 leads to dry-out and salt precipitation in the near well zone and a maximum permeability reduction of 24%. After abandonment, brine flows towards the well, resulting in redissolution of precipitated salt, leading to salt saturated brine in the near-well bore area. After 1,000 years, it is predicted that supersaturated brine is concentrated in the lower part of the reservoir, where solid salt still remains. The computed long-term effects of brine mobility could influence predictions of well-cement degradation and well-abandonment strategies like intentional clogging.

INTRODUCTION

Depleted gas reservoirs are potential sinks for CO_2 in The Netherlands, thereby reducing atmospheric CO_2 (Benson and Cook, 2005). The offshore P18 gas field in the North Sea is a very good candidate for future CO_2 injection, because of its location (close to CO_2 point sources), infrastructure, and reservoir maturity (Arts et al., accepted). Sufficiently high CO_2 injection rates are required for making Carbon Capture, Utilization, and Storage (CCUS) economically attractive for oil and gas operators, while long-term integrity of the whole storage complex is important for license applications. It is therefore important to understand the behavior of the reservoir during and after CO_2 injection.

It is known that salt precipitation can hamper the productivity in gas producing fields (Kleinitz et al., 2003) or the injectivity in natural gas storage aquifers (Lorenz and Müller, 2003). It is also predicted that salt precipitation could reduce the permeability when injecting supercritical CO_2 (SC-CO_2) in saline aquifers (e.g. Pruess and Müller, 2009; Müller et al., 2009; Alkan et al., 2010; André et al., 2007) and depleted gas fields (Giorgis et al., 2007). The physical mechanisms affecting dryout and salt precipitation in saline aquifers are described by Pruess and Müller (2009). Most of these mechanisms also hold for depleted gas fields, although brine displacement by SC-CO_2 away from the well is expected to be less dominant in depleted gas fields due to the (lower) brine relative permeability.

Salt precipitation due to water evaporation into injected dry SC-CO_2, followed by capillary backflow, is demonstrated both in core plug experiments (Ott et al., 2011) and in several modeling studies (e.g., Pruess and Müller, 2009; Müller et al., 2009; Alkan et al., 2010; André et al., 2007; Giorgis et al., 2007; Ott et al., 2011). It was found that brine capillary backflow will have a larger impact when the CO_2 injection rate is lower (Pruess and Müller, 2009), and thus the injection rate should be high enough to avoid injectivity problems (Giorgis et al., 2007). It was also concluded that the saturation gradient and local salt precipitation are determined by water evaporation kinetics. These kinetics are currently not taken into account in TOUGH2

(and other simulators), as discussed by Ott et al. (2011). Thus, modeling the precise impact of capillary backflow during CO_2 injection carries uncertainties.

The initial water saturation (S_w) as a function of reservoir depth also has uncertainties. The S_w is commonly measured during drilling of a well using a logging tool (Rider, 2006), and depends on the various petrophysical properties of all (sandstone) layers and the height above the free water level. The heterogenic character of reservoirs usually makes an accurate description of the petrohysical properties and S_w very difficult, but these properties determine the brine mobility in the reservoir. This mobility is important for CO_2 injection, as demonstrated by Giorgis et al. (2007) showing two cases: mobile and immobile brine. Long-term brine mobility has received much less attention than short-term brine mobility. However, long-term effects could influence well-cement degradation and intentional clogging after well-abandonment (Wasch et al., 2012).

The aim of this work is to simulate effects in the near-well zone of a theoretical reservoir, based on characteristics of the P18 gas field in the Dutch offshore. We focus on the effect of gas production and CO_2 injection on brine flow and salt precipitation.

METHODS

Model setup

The model consists of four geological layers with varying petrophysical properties, as determined from well logs (Table 1). In addition, the salt mass fraction (X_{NaCl}) is 0.1, the reservoir temperature (T) is 90ºC, and the initial (average) gas pressure ($P_{gas,i}$) is 375 bar. Figure 1 shows a 2D window of the radial model setup.

In the horizontal direction, 50 grid cells are imposed per layer with grid refinement (factor of 1.05) in the vicinity of the well. The model has a radius of 1,000 m. In the vertical direction, 80 grid cells are imposed with grid refinement (factor of 1.2) at the upper and lower boundaries of each deposit. Gas production and CO_2 injection were not considered for the VP Formation (Fm) due to its tight properties (Table 1), although it was taken into account for computing the equilibrium brine and gas distribution. The FWL is located at the bottom of the VP Fm, but is not considered an active aquifer. This means that the depth of the FWL does not change upon production and injection.

Table 1. Petrophysical characteristics of the geological deposits in the model: thickness (Δz), porosity (φ), and permeability (k). The number of vertical cells per deposit is also given.

Geological deposit	Δz (m)	φ (-)	k (mD)	cells (-)
Hardegsen (HD) Fm	26	11	154	10
Upper Dethfurt (UD) Mb	50	9	38.5	20
Lower Dethfurt (LD) Mb	22	7	30.6	10
Volpriehausen (VP) Fm	113	3	0.21	40

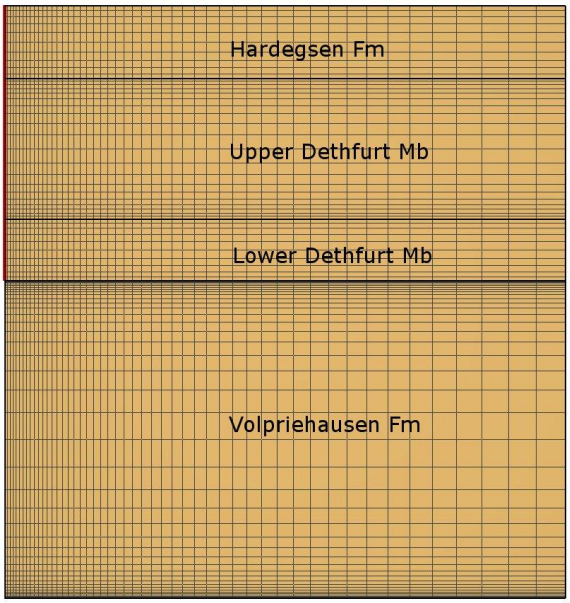

Figure 1. 2D window of the radial model with four geological layers (Petrasim interface). The injection well is located at the left side and does not penetrate the VP Fm.

Capillary pressure and relative permeability

For the capillary pressure and relative permeability curves, a correlation was used with the porosity and height above the FWL ($\Delta h = h - h_{FWL}$) as main parameters. The van Genuchten equations are used to parameterize these curves, as shown in Figure 2 and Figure 3, respectively. The parameters used in these equations are derived from a best fit to the curves used in other work (Arts et al., accepted).

The relative permeability depends on the rock, fluids, and thermodynamic conditions (Krevor et al., 2012). It is commonly believed that the relative permeability is determined by the wettability of the sandstone. Here it is assumed that the wettability and therefore relative permeability of CH_4 and CO_2 is similar. Hysteresis effects were not taken into account in this study.

For a two-phase system, the standard output of the TOUGH2 simulator reports the gas pressure (P_{gas}) and the capillary pressure (P_{cap}). The brine pressure (P_{brine}) can be computed using:

$$P_{brine} = P_{gas} - |P_{cap}|.$$

The formula given above shows the absolute value of P_{cap}, because its definition depends on the simulator (in TOUGH2, P_{cap} is defined negative for drainage). In case of static equilibrium, P_{cap} can also be computed using the difference in brine density (ρ_{brine}) and gas density (ρ_{gas}), the gravitational constant (g), and Δh:

$$P_{cap}(S_w) = (\rho_{brine} - \rho_{gas}) g \Delta h.$$

P_{cap} as a function of S_w depends on the type of gas that is present. Scaling of P_{cap} can be done using the dimensionless Leverett J-function (Leverett, 1941), which is commonly used in the oil and gas industry:

$$J(S_w) = \frac{P_{cap}(S_w)\sqrt{\left(\frac{k}{\varphi}\right)}}{\sigma \cos\theta}.$$

Both J and P_{cap} are given as a function of S_w, σ is the interfacial tension and θ is the contact angle. If we assume that θ is similar for CO_2 and CH_4, we can approximate $P_{cap,CO2}$ using $P_{cap,CH4}$ by

$$P_{cap,CO2}(S_w) = \frac{\sigma_{b,CO2}}{\sigma_{b,CH4}} P_{cap,CH4}(S_w),$$

where $\sigma_{b,CO2}$ and $\sigma_{b,CH4}$ are the brine-CO_2 and brine-CH_4 interfacial tensions, respectively. At high pressure, $\sigma_{b,CO2}$ is smaller than $\sigma_{b,CH4}$ because of the larger affinity of CO_2 to water (Fleury et al., 2010). Reported values of $\sigma_{b,CO2}$ are on the order of 30 mN/m (Fleury et al., 2010; Chalbaud et al., 2010; Saeedi and Rezaee, 2012), while $\sigma_{b,CH4}$ is on the order of 45 mN/m (Saeedi and Rezaee, 2012). For this reason, the curves in Figure 3 are scaled with a factor of 0.667 for CO_2. In this study, it is assumed that σ and θ are independent of pressure.

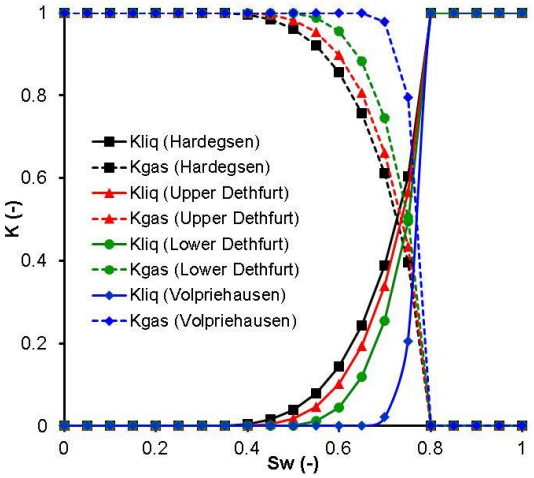

Figure 2. Relative permeability (K) of gas (K_{gas}) and liquid (K_{liq}) for the four geological deposits, used for both CH_4-brine and CO_2-brine.

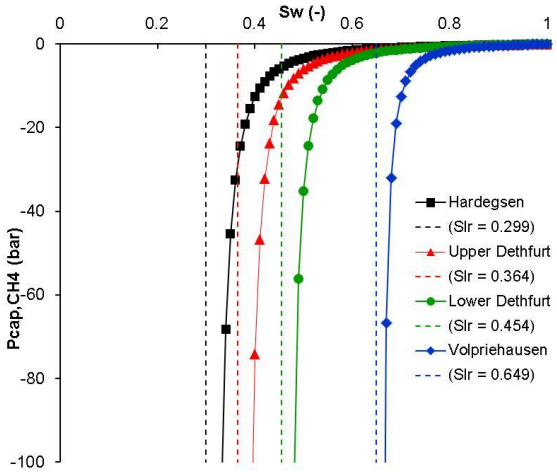

Figure 3. Capillary pressure ($P_{cap,CH4}$) as a function of the water saturation (S_w) for the four geological deposits. $P_{cap,CO2}$ is derived by scaling $P_{cap,CH4}$ with a factor of 0.667. The residual water (S_{lr}) asymptote is also given. $P_{cap,max}$ is 100 bar.

Equilibrium gas and brine saturation

On a geological time scale, upward gas migration into permeable sandstone layers led to brine drainage and lowering of the FWL. The brine that was left behind, due to capillary forces, is the current water saturation and is usually measured with a logging tool (Rider, 2006). The mobility through the VP Fm is relatively low due to its tight properties. In general, other impermeable (shale) layers in the more permeable deposits could also have retarded the brine mobility.

In this study it is assumed that S_w is in hydrostatic equilibrium with the FWL. Below, we describe the workflow how to compute S_w as a function of depth, using the estimated capillary pressure (drainage) curves (Figure 3) and TOUGH2-EWASG (see gas production). The relative permeability of gas and brine were set to perfectly mobile brine (K_{liq}=1 and K_{gas}=1), for speeding up the calculations. A dummy layer on top of the HD Fm is included and serves as a gas inlet (see below). The dummy layer has a thickness of 1.0 cm, which is relatively small compared to the reservoir thickness. In this way it has a negligible effect on the (computed) hydrostatic pressure. The capillary pressure of the dummy layer is set to zero. The three-step workflow is as follows:

1) Hydrostatic equilibrium: The model given in Figure 1 is fully gas-saturated with gas and the average pressure (P_{gas}=375 bar) is assigned. Accordingly, the hydrostatic pressure is computed by TOUGH2, showing a linear relation as a function of depth.

2) Brine and gas distribution: The computed pressure from the previous step is initialized using the SAVE file. All cells in the layers are now assigned fully water-saturated, except the dummy layer. The dummy layer and the bottom layer are assigned as fixed (infinitely large volume), the latter to represent the FWL. Using these constraints, water can flow out at the bottom of the reservoir and gas can flow in from the top of the reservoir. In this way the initial and final hydrostatic pressure is maintained.

3) Equilibrium check: The final conditions of the previous step are initialized using the SAVE file. The dummy layer is removed and the bottom (FWL) layer is unfixed, to check whether the conditions are in equilibrium without constraints.

The results define the equilibrium brine and gas saturation before production.

Salt precipitation

Both gas production and CO_2 injection were simulated using TOUGH2 modules that can handle precipitation of solid salt and permeability reduction (see below). We used a tubes-in-series porosity-permeability model (Verma and Pruess, 1988) with a fractional length of pore bodies (Γ=0.8) and a fraction of original porosity (φ_r=0.8) for which k=0. In practice this means that a salt occupancy of 20% pore volume completely clogs the formations.

Gas production (TOUGH2-EWASG)

We computed the brine mobility during gas production to study whether the computed initial S_w would change. We modeled production from the upper three geological deposits with TOUGH2-EWASG (Battistelli et al., 1997), which was developed for geothermal applications. It can handle a three-phase mixture of water, NaCl, and several non-condensable gases (including CH_4). One disadvantage is that real gas properties are not properly modeled. Gas dissolution is described by Henry's law, with coefficients that depend on the temperature and salinity. EWASG also has an enthalpy limitation (Lorenz and Müller, 2003), but isothermal conditions are imposed in this study.
A constant rate of 0.12 Mton/year is used with a production time of 23.9 years, implying a total production of 2.88 Mton and a depletion pressure (P_{depl}) of 26.6 bar. As mentioned above, the relative permeability (Figure 2) and capillary pressure (Figure 3) are both used.

CO_2 injection (TOUGH2-ECO2N)

After gas production, CO_2 is injected at fixed T (i.e., 90°C) with a constant rate of 1.01 Mton/year for 11.3 years and thus a total CO_2 amount of 11.4 Mton. At a final (average) pressure of 375 bar, the average density of CO_2

(770 kg/m^3) is approximately four times higher than the (ideal) density of CH_4 (200 kg/m^3), which explains why the injected amount of CO_2 is four times larger than the produced amount of CH_4 for returning to the initial pressure.

Injection of CO_2 is carried out with TOUGH2-ECO2N, which describes two-phase flow in the H_2O-salt-CO_2 system. Dissolution of CO_2 in brine and water evaporation in CO_2 is described using equations of state (EOS). ECO2N does not take into account CH_4 and it is assumed that all initial gas consists of CO_2. Hence, the distribution of CO_2 and CH_4 in the reservoir is not modeled. For example, this can be done with TOUGH2-EOS7c (Oldenburg et al., 2001; Audigane et al., 2008) and is of special interest when modeling enhanced gas recovery (EGR). Modeling of salt precipitation cannot be done with TOUGH2-EOS7c.

The final conditions after gas production were initialized using the SAVE file, thereby replacing all CH_4 gas into CO_2. The properties of both gases are different at the given conditions (T=90ºC, P_{depl}=26.6 bar, X_{NaCl}=0.1). However, the differences we computed are less than 1%, e.g., CH_4 and CO_2 solubility in brine and water vapor in gas. Modeling the impact of capillary backflow during CO_2 injection involves uncertainties (see introduction). We therefore assumed immobile brine (K_{liq}=0 and K_{gas}=1) during continuous CO_2 injection, thereby preventing capillary backflow and enhanced salt precipitation.

Table 2. Overview of computed produced amounts of gas and liquid

component	water		methane	
phase	gas	liquid	gas	diss.
initial (Mton)	0.01	11.79	3.07	0.04
final (Mton)	0.01	11.77	0.21	<0.01
produced (Mton)	<0.01	0.02	2.86	0.03
produced (%)	0.8	0.2	93.1	93.1

Long-term effects

After closing the injection well, the simulations are continued up to 1,000 years. The long-term effects of brine flow (including capillary flow) on precipitated salt are computed. Molecular diffusion was neglected in this study, although this could influence salt gradients.

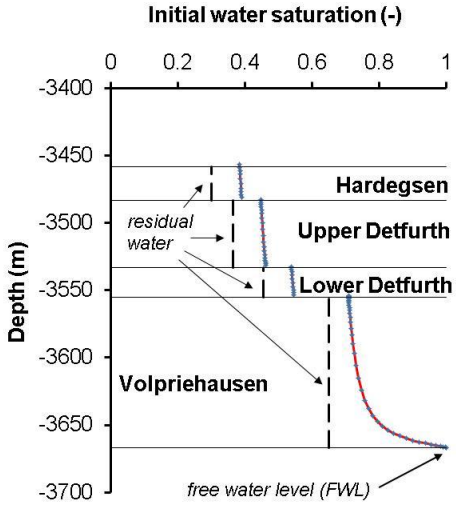

Figure 4. Water saturation (S_w) in the gas field before production. Dashed lines indicate the residual water (S_{lr}), as used in the Van Genuchten relative permeability (Figure 2) and capillary pressure (Figure 3).

RESULTS

Equilibrium water saturation

We followed the scheme mentioned above to compute P_{gas} and P_{cap} as a function of depth using TOUGH2. $|P_{cap}|$ is 0 at the FWL and increases with increasing height above the FWL, up to 17.5 bar at the top of the HD Fm. The computed P_{cap} is directly translated by TOUGH2 into an equilibrium S_w using the curves given in Figure 3. The S_w as a function of depth is given in Figure 4. The S_w in the VP Fm is relatively large, because the deposit has a low porosity and the FWL is located at the bottom. The S_{lr} and initial S_w decrease with increasing porosity in the upper parts of the reservoir up to 11% for the HD Fm (Table 1). As mentioned in the methods section, the S_{lr} is assumed to be similar for both CH_4 and CO_2.

Gas production

Table 2 shows the amounts of water (0.02 Mton) and methane (2.86 Mton) that are produced during 24 year of gas production, which correspond to 0.8% and 93.1% of the initial amounts present. This means that relatively small amounts of water are produced, and the mobility of water is low, owing to the relative

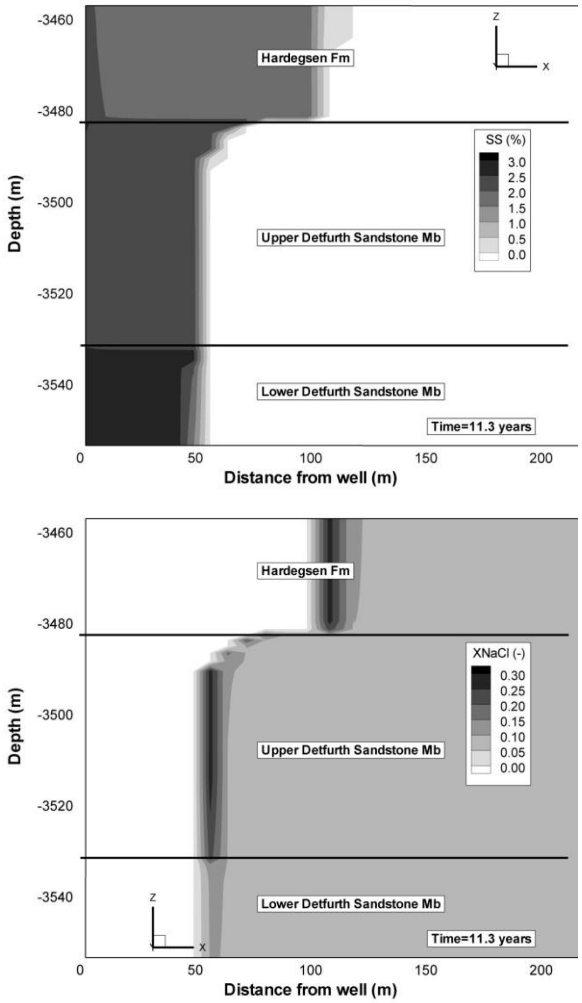

Figure 5. Pore volume percentage (SS) occupied by solid salt (top) and X_{NaCl} (bottom) in the near-well area, after closing the injection well.

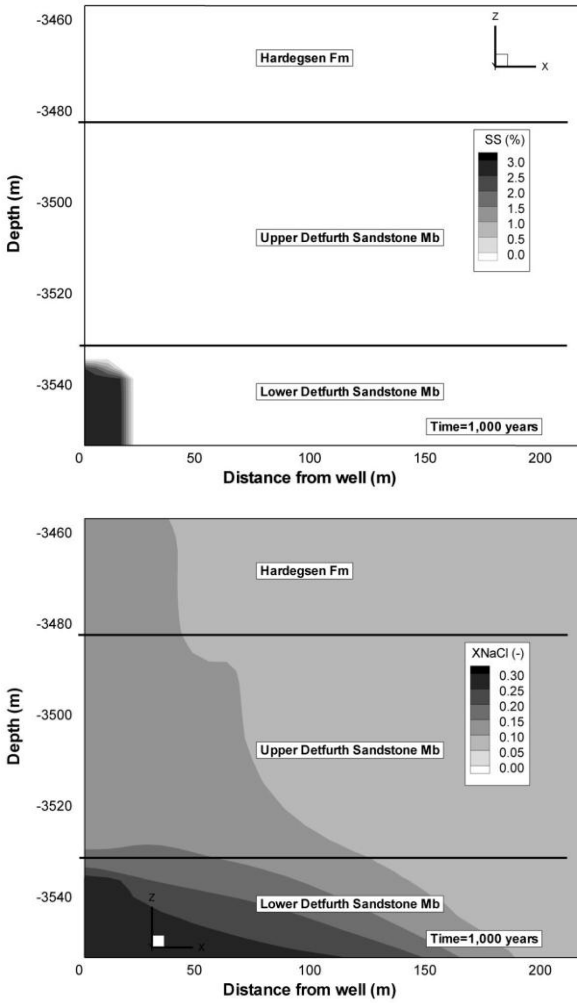

Figure 6. Pore volume percentage (SS) occupied by solid salt (top) and X_{NaCl} (bottom) in the near-well area, 1,000 years after closing the injection well.

permeability. Computed water saturations are 0.05 to 0.1 higher than the residual water saturation (Figure 4), but the corresponding water mobility is low (K_{liq}<0.015; Figure 2). In addition, the maximum computed pressure drawdown is only a few bars. Generally, the drawdown depends on operational constraints, including economics.

Under standard temperature and pressure (NTP) conditions (i.e., T=15.6°C and P=1 bar) the densities of CH_4 and brine are ~0.717 kg/m^3 and 1066 kg/m^3, respectively. The corresponding produced volumes are 0.022 Mm^3 of water and 4330 Mm^3 of gas, indicating that a very small water volume is produced compared to gas volume. Salt precipitation was not observed, most probably due to a relatively low salinity as compared to other studies involving CH_4 (Lorenz and Müller, 2003).

CO_2 injection

Water evaporation in the near-well area was modeled during CO_2 injection, with salt precipitation as a result (Figure 5). The results show that the dryout radius ranges from 53 m (LD Mb) to 113 m (HD Fm). Salt precipitation is modeled from to 2.2% (HD Fm) up to 2.8% (LD Mb) of the pore volume, corresponding to *k*-reductions with 19% and 24%, respectively. These values depend on the characteristics of the tubes-in-series model and uncertainties exists. At the front of the dryout zone, a small zone with increased salinity up to salt-saturation

(X_{NaCl}=0.272) is predicted. The assumption of immobile brine prevented imbibition into the dry-out zone during injection (see Methods).

Long-term effects

After closing the injection well, brine mobility in the reservoir was modeled, resulting in brine flow into the dryout zone (Figure 6). After 1,000 years, most of the precipitated salt dissolved, except for 21 m around the well in the LD Mb at the bottom of the reservoir. In addition, the salinity in the whole near-well bore area increased, but is salt saturated in the LD Mb. These differences are potentially caused by two effects. First, the solid salt in the LD Mb is more concentrated, the dryout zone is smaller, and dissolution is expected to take more time. The brine flow rate into the LD Mb should also be considered. Second, the brine density increases with increasing salinity, resulting in a gravitational flow. Salt undersaturated brine is flowing laterally into the near-well bore area in the upper region of the reservoir (especially in the HD Fm). Then it becomes heavier and migrates into the lower parts of the reservoir, where it starts migration away from the near-well area along the boundary with the VP Fm. These mechanisms retard the solid salt dissolution in the LD Mb, compared to other (more shallow) deposits.

Hysteresis in the capillary pressure was not taken into account, and hence only drainage curves were used (Figure 3). Wetting of the dryout zone should have been considered with an imbibition parameterization. At similar capillary pressure in reservoir rock, imbibition usually corresponds to lower S_w as compared to drainage (Leverett, 1941). For the current study, this would result in a lower S_w of the dryout zone and less faster salt dissolution.

CONCLUSIONS

This paper discusses the effect of gas production and CO_2 injection on brine flow and salt precipitation, using characteristics based on the P18 field in the offshore part of The Netherlands. We computed the initial S_w, assuming equilibrium on a geological time scale, showing mobile water. However, the amounts of production water are relatively small when gas is produced from the field. No salt precipitation was observed.

We assumed immobile brine during CO_2 injection. The results show dryout and salt precipitation in the near-well area and larger amounts of salt in the lower part of the reservoir, compared to the upper part of the reservoir. Permeability reductions up to 24% are expected in the reservoir during CO_2 injection. Capillary backflow of brine was allowed after the closing the well, showing redissolution of salt and induced gravitational flow in the near-well area. Occurrence of solid salt is still predicted in the lower part of the reservoir after 1,000 years, as well as saturated brine. These effects could influence predictions of well-cement degradation and well-abandonment strategies like intentional clogging.

ACKNOWLEDGMENT

This work was carried out in the framework of the Dutch CATO-2 program. The authors are grateful to the Dutch Ministry of Economic Affairs and sponsoring companies for funding. We thank Laura Wasch, Kees Geel, Saskia Roels, and Alfredo Battistelli for helpful discussions.

CITATIONS

Alkan, H., Y. Cinar, and E.B. Ülker, Impact of Capillary Pressure, Salinity and In situ Conditions on CO2 Injection into Saline Aquifers, Transp. Porous Media, 84(3), 799-819, 2010.

André, L., P. Audigane, M. Azaroual, and A. Menjoz, Numerical modeling of fluid-rock chemical interactions at the supercritical CO2-liquid interface during CO2 injection into a carbonate reservoir, the Dogger aquifer (Paris Basin, France), Energy Convers. Manage., 48(6), 1782-1797, 2007.

Arts, R.J., C. Hofstee, V.P. Vandeweijer, M.P. Pluymaekers, D. Loeve, and A. Kopp, CO2 storage in the depleted P18-4 gas field offshore the Netherlands (the ROAD project), Int. J. Greenhouse Gas Control, accepted.

Audigane, P., J. Lions, I. Gaus, C. Robelin, P. Durst, C.M. Oldenburg, T. Xu, B.v.d. Meer, and K. Geel, Geochemical modeling of CO2 injection into a methane gas reservoir at the K12-B field, North Sea, In: Carbon dioxide sequestration in geological media - State of

the science, Eds. M. Grobe, J.C. Pashin and R.L. Dodge. AAPG Studies 59, 1-20, 2008.

Battistelli, A., C. Calore, and K. Pruess, The simulator TOUGH2/EWASG for modelling geothermal reservoirs with brines and non-condensible gas, Geothermics, 26(4), 437-464, 1997.

Benson, S. and P. Cook, Underground geological storage, In: IPCC Special report on carbon dioxide capture and storage, Chapter 5. Intergovernmental Panel on Climate Change, Eds. B. Metz, O. Davidson, H. De Coninck, M. Loos and L. Meyer. Cambridge University Press, 431, 2005.

Chalbaud, C., M. Robin, J.-. Lombard, H. Bertin, and P. Egermann, Brine/CO2 interfacial properties and effects on CO2 storage in deep saline aquifers, Oil Gas Sci. Technol., 65(4), 541-555, 2010.

Fleury, M., J. Pironon, Y.M. le Nindre, O. Bildstein, P. Berne, V. Lagneau, D. Broseta, T. Pichery, S. Fillacier, M. Lescanne, and O. Vidal, Evaluating sealing efficiency of caprocks for CO2 storage: An overview of the geocarbone-integrity program and results, Oil Gas Sci. Technol., 65(3), 435-444, 2010.

Giorgis, T., M. Carpita, and A. Battistelli, 2D modeling of salt precipitation during the injection of dry CO2 in a depleted gas reservoir, Energy Convers. Manage., 48(6), 1816-1826, 2007.

Kleinitz, W., G. Dietzsch, and M. Köhler, Halite scale formation in gas-producing wells, Chem. Eng. Res. Des., 81(3), 352-358, 2003.

Krevor, S.C.M., R. Pini, L. Zuo, and S.M. Benson, Relative permeability and trapping of CO_2 and water in sandstone rocks at reservoir conditions, Water Resour. Res., 48(2), 2012.

Leverett, M.C., Capillary behaviour in porous solids, Transactions of the AIME, 142, 159-172, 1941.

Lorenz, S. and W. Müller, Modelling of halite formation in natural gas storage aquifers. Proceedings TOUGH Symposium 2003, Lawrence Berkeley National Laboratory, Berkeley, California, May 12–14, 2003.

Müller, N., R. Qi, E. Mackie, K. Pruess, and M.J. Blunt, CO2 injection impairment due to halite precipitation, Energy Procedia, 1(1)9th International Conference on Greenhouse Gas Control Technologies, GHGT-9, Washington DC, 3507-3514, 2009.

Oldenburg, C.M., K. Pruess, and S.M. Benson, Process modeling of CO2 injection into natural gas reservoirs for carbon sequestration and enhanced gas recovery, Energy Fuels, 15(2), 293-298, 2001.

Ott, H., K.D. De Kloe, F. Marcelis, and A. Makurat, Injection of supercritical CO2 in brine saturated sandstone: Pattern formation during salt precipitation, Energy Procedia, 410th International Conference on Greenhouse Gas Control Technologies, Amsterdam, 4425-4432, 2011.

Pruess, K. and N. Müller, Formation dry-out from CO_2 injection into saline aquifers: 1. effects of solids precipitation and their mitigation, Water Resour. Res., 45(3), 2009.

Rider, M.H., The Geological Interpretation of Well Logs. 2nd edition, Progress Press Co Ltd., Malta, 2006.

Saeedi, A. and R. Rezaee, Effect of residual natural gas saturation on multiphase flow behaviour during CO 2 geo-sequestration in depleted natural gas reservoirs, J Pet Sci Eng, 82-83, 17-26, 2012.

Verma, A. and K. Pruess, Thermohydrological conditions and silica redistribution near high-level nuclear wastes emplaced in saturated geological formations, J. Geophys. Res., 93(B2), 1159-1173, 1988.

Wasch, L.J., J. Wollenweber, and T.J. Tambach, A novel concept for long-term CO_2 sealing by intentional salt clogging, Proceedings TOUGH Symposium 2012, Lawrence Berkeley National Laboratory, Berkeley, California, September 17-19, 2012.